Improving the sound absorption performance of sustainable thermal insulation materials: Natural hemp fibres.

Andrea Santoni[a,*], Paolo Bonfiglio[b], Patrizio Fausti[a], Cristina Marescotti[a], Valentina Mazzanti[a], Francesco Mollica[a], Francesco Pompoli[a]

[a]*Department of Engineering, University of Ferrara, via G. Saragat 1, 44122 Ferrara, Italy*
[b]*Materiacustica s.r.l., via Ravera 15/A, 44122 Ferrara, Italy*

Abstract

Compared to the traditional synthetic fibrous materials, natural fibres represent sustainable solution to be used either in building construction and noise control engineering and acoustic treatments. Natural fibres are mainly employed in the building industry for their hygrothermal properties, however the possibility to also use them for acoustic purposes would greatly increase their appeal to the market. While synthetic fibres have been studied for almost fifty years, the knowledge of natural fibres is still limited and needs to be expanded. Natural fibres are affected by a large variability of the physical properties, which consequently causes great uncertainty in numerical modelling and difficulties during the design process of acoustics treatments. This study highlights the possibility to enhance the acoustic performance of hemp fibrous materials through the manufacturing process, investigating how each treatments affects the material's physical characteristics and its sound absorption coefficient. Moreover, a simplified model to evaluate the acoustic performance of hemp fibrous materials as a function of their density is proposed, in order to provide a practical tool to investigate and compare different solutions. The physical parameters numerically evaluated for a varying compression rate have been compared with the experimental results, measured at each stage of the production process on samples with a different density and thickness. The global reliability of the proposed approach is finally investigated by comparing the experimental sound absorption for normal incidence with the results obtained from the Johnson-Champoux-Allard model.

Keywords: natural-fibres, sustainable building industry, hemp-fibrous material, sound absorption coefficient, material characterisation

1. Introduction

As sound insulation and noise control have become a primary concern in many industrial fields, several porous and fibrous materials have been developed, by using polymers and petroleum-based products. In recent years, in an attempt to reduce energy consumption in order to encourage sustainable development and preserve resources for future generations, sustainable materials and

*Corresponding author
Email address: andrea.santoni@unife.it (Andrea Santoni)

their application have been increasingly studied. The sustainability of a material is generally considered in terms of resources usage, environmental impact, human health, and social equity. Moreover, the production process should require the least amount of energy consumption – green energy is preferable to non-renewable resources – and have the minimum manufacturing waste, or provide second life options for the waste products. Besides traditional petroleum-based materials such as melamine and polyurethane foams, or polyester fibres, there are other materials, commonly used for hygrothermal and acoustic treatments, which need to be sealed although they are derived from natural or recycled products, since they may contain substances impacting on human health if they come into contact with the skin or are inhaled. On the other hand, natural materials such as wood, coconut, kenaf and hemp fibres, obtained from renewable resources by means of a manufacturing process with a reduced impact on the environment [1], are also harmless for human health, since they do not contain toxic substances [2, 3]. For these reasons, compared with traditional materials employed to improve the thermal and acoustic performances in buildings, natural fibres represent an eco-friendly sustainable solution. Natural fibres, such as hemp and kenaf, have been thoroughly studied and used for different applications in building construction [4]. For example in fibre-reinforced concrete or other bio-composites [5]and especially as fibrous thermal insulation materials [6]. Several studies can be found in the literature regarding both the characterisation of hygrothermal and physical properties of these fibres [7, 8] and their applications [9, 10, 11]. Recent studies have shown that natural fibres can also be employed for both for noise control applications providing either a good sound insulation or sound absorption performance [12, 13, 14, 15]. However, a systematic characterisation of their acoustic behaviour is still lacking. Nevertheless, the possibility to also provide an adequate acoustic performance by employing natural fibres, would certainly increase the market interest, helping to move towards a more sustainable building industry. Nowadays in fact, multi-purposes solutions are commonly implemented in building construction, providing for example thermal and acoustic protection [16], or combining light shading with thermal and noise protection [17, 18].

In the literature several acoustic models to investigate different kinds of fibrous materials can be found. The most widely used empirical model for mineral and glass wool is probably the one developed by Delany and Bazley [19, 20]. Other models have also been developed in order to investigate different fibrous, porous or granular materials, like, for example, the widely used Johnson-Champoux-Allard equivalent fluid model [21, 22], or the alternative six-parameter model proposed by Lafarge [23], or again the model specifically developed for polyester fibres by Garai and Pompoli [24]. While conventional fibrous materials have been thoroughly investigated and the physical parameters which affect their acoustic performance are well known, the knowledge of the physical characteristics of natural fibrous materials and their possible influence on their acoustic performance is still limited. Moreover, an optimisation of the manufacturing process of natural fibres in order to increase their acoustic performance has never been investigated. Being generally produced in a lower amount compared to synthetic fibres, either by small enterprises, or sometimes even in artisan workshops, natural fibres are characterised by a significant variability of their diameter and other physical properties. The fact that the fibres' diameter distribution cannot be arbitrarily controlled like in the production process of synthetic fibres represents an issue for the evaluation of their acoustic performance, since all the acoustic models have been developed for homogeneous fibrous materials with a constant diameter [25, 26].

In this study an experimental investigation on the variety *Liptko* of the plant species *Cannabis Sativa* has been performed. Only few studies, recently published, on the characterisation of hemp fibres can be found in the literature [27, 28]. The aim of this work is to investigate some aspects which, to the authors' best knowledge, have never been analysed before for this kind of fibrous material, even though they may have a significant influence on its acoustic behaviour. As was observed, rough hemp-fibrous materials exhibited a relevantly lower sound absorption compared to synthetic materials such as polyester fibres. Therefore, the influence that the different stages of the manufacturing process have on the physical characteristics and how those affect the material's sound absorption have been analysed, in order to define the mechanical and chemical treatments that optimises the acoustic performance of such eco-friendly material. Furthermore, we propose a simplified approach to characterise the physical parameters of hemp-fibrous material, which requires the evaluation of its sound absorption coefficient, based on the knowledge of the effective fibres' radius and of the material's apparent density. The methodology makes use of a fluid dynamic model [29] to determine, from the experimental air flow resistivity, the effective radius of the equivalent homogeneous fibrous-material. Moreover, from the air flow resistivity and the absorption coefficient for normal incidence of the hemp fibrous material, measured at a given compression rate, it is possible to define all the macroscopic parameters [30] required as input data in the Johnson-Champoux-Allard (JCA) acoustic model. From this initial set of parameters, defined for a given density and thickness, the proposed methodology, inspired by Castagnède's model [31], allows to investigate the material's physical parameters and consequently the sound absorption coefficient for any compression rate. The method was validated by comparing the numerical results evaluated at four different stages of the manufacturing process with the experimental data. In the next section the investigated material is introduced and the different stages of the manufacturing process are described. In section 3 the basics of Johnson-Champoux-Allard model are summarised. The methodology proposed to characterise the material's physical parameter is given in detail in section 4, while the main results are validated and discussed in section 5.

2. Material and manufacturing process description

The investigated hemp material, provided by EmilCanapa s.r.l. (Reggio Emilia, Italy), was of the species Cannabis Sativa L and Lipko variety. The innermost part of the hemp stems, often referred to as the pith, is surrounded by woody-fibres known as hurds or shives. The outermost layer, which encloses the hurds, is constituted by bast fibres. These are the fibres that were used in this investigation. After harvesting, the leaves were manually separated from the hemp stems, which were macerated in the field for two months. Subsequently, the hemp stems were worked first with a farm shredder and then with a rotary sieve to divide the bast fibres from the hurds. These separated fibres subsequently underwent four treatments:

1. **01.CAR – Carding:** this mechanical process is performed in order to break down and untangle long fibres and to remove the remaining traces of dirt and the shortest fibres [32].
2. **02.NaOH – Alkaline treatment ($5\%/h$):** : the fibres are soaked in a 5 wt.% sodium hydroxide (NaOH) solution at room temperature for 60 minutes. After treatment, the fibres were washed with distilled water, neutralized with 1 wt.% acetic acid solution, and then dried overnight in a vacuum oven at T = 80°C. This chemical treatment removed non-cellulosic components and facilitated the extraction of the fibrils, thus improving quality of the fibres [33, 34].
3. **03.WTC – Wide tooth combing:** a wide tooth comb is used in order to align the fibres, open the fibre bundles and release the fibrils thanks to the shearing stresses induced by the combing process.

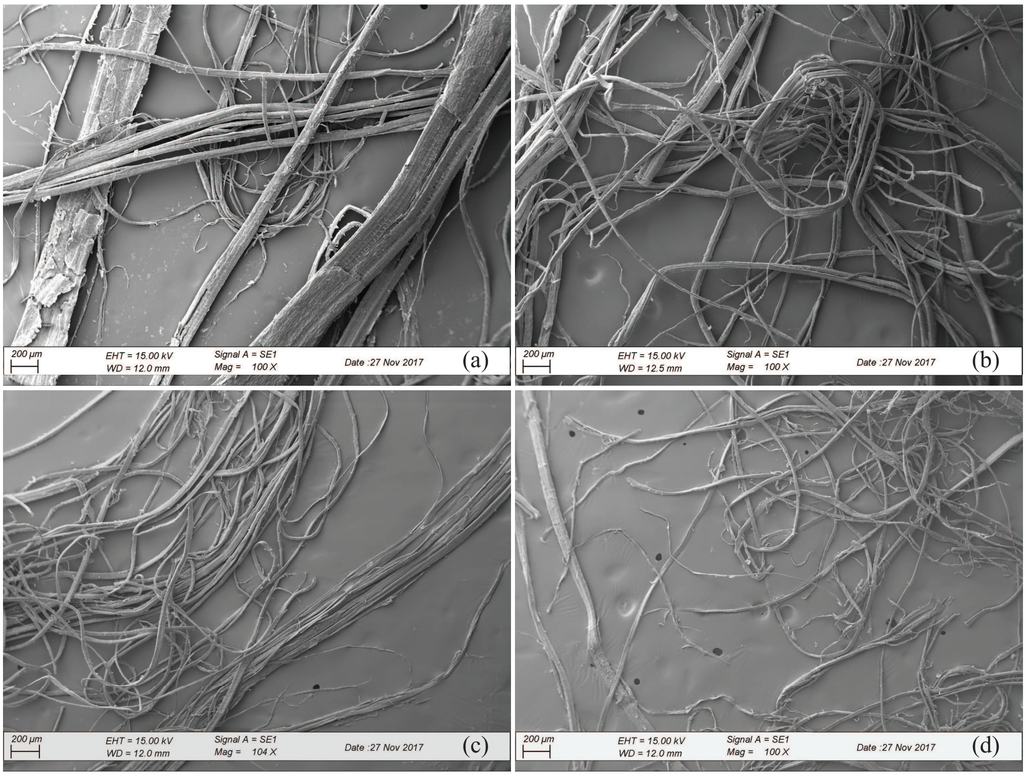

Figure 1: SEM images of hemp fibres: a) hemp fibres after carding process: 01.CAR; b) hemp fibres after alkaline treatment: 02.NaOH; c) hemp fibres after wide tooth combing: 03.WTC; d) hemp fibres after fine tooth combing: 04.FTC.

4. **04.FTC – fine tooth combing:** this last mechanical process is a further refinement of the previous step 03.WTC; in this case a fine tooth comb is used instead of the wide tooth one.

After each step of the manufacturing process, samples of hemp fibres were collected and sputter-coated in gold in order to be analysed by a scanning electronic microscopy (SEM). A SEM ZEISS EVO M15 microscope with accelerating voltage of 15 kV was used. Figure 1 shows how each stage of the manufacturing process drastically changed the fibres' morphology. Raw hemp fibres exhibited a complex hierarchical structure constituted by bundles of fibrils glued together by an interphase consisting mainly of non-cellulosic components. The alkalization (02.NaOH) combined with mechanical treatments (03.WTC and 04.FTC) removed such cementing substances, unveiling the fibres. For this reason, a significant reduction of the mean diameter of the fibres is shown from step 01.CAR to step 04.FTC, and the amount of fibre bundles decreases [35]. Even though, for all four materials a large dispersion was found in diameters distribution, as shown in Figure 2. Therefore, the determination of a weighted averaged radius [36] is non-trivial and it would certainly be affected by a significant uncertainty. The average radius can be used to compute the physical parameters of a fibrous material. However, an uncertain estimation would provide highly inaccurate results.

Published article available online: https://doi.org/10.1016/j.apacoust.2019.02.022

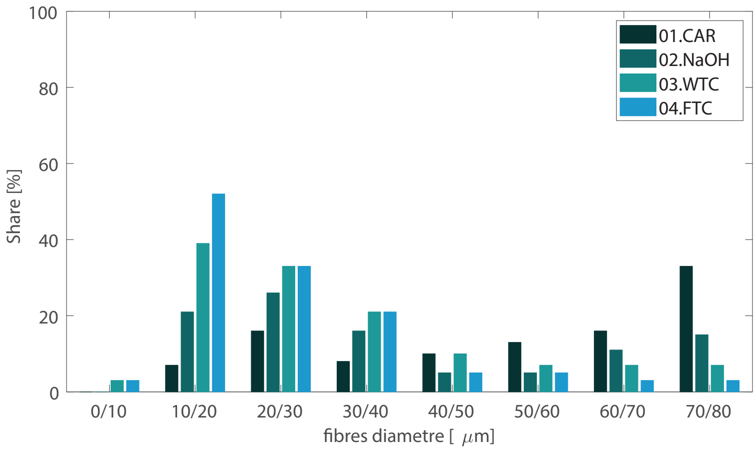

Figure 2: Diameter distribution of hemp fibres after each manufacturing process.

3. Acoustical model for sound absorption

For a great variety of fibrous and porous materials excited by an incident acoustic wave, it is possible to assume their solid frame to be rigid, either due to the high value of the elastic modulus, or the high density, or again because of special test conditions. These media can be described as equivalent fluids, characterised by an effective density ρ and an effective bulk modulus K. The well known Johnson-Champoux-Allard (JCA) equivalent fluid model [21, 22] describes visco-inertial and thermal dissipative effects inside a porous material having a rigid and motionless frame. Such model involves, in the computation of the effective density ρ and the effective bulk modulus K, five macroscopic parameters:

- *airflow resistivity* - σ [Ns/s^4]: it is the resistance of the material to an airflow passing through it. Airflow resistivity is determined as:

$$\sigma = \frac{\Delta p}{h v_{airflow}} \tag{1}$$

  where Δp is the pressure drop across the medium while $v_{airflow}$ is the airflow rate passing through the medium of thickness h.

- *open porosity* - ϕ [$-$]: it represents the fractional amount of air volume within the interconnected pores in the medium. It can be evaluated as the ratio between the air volume V_{fluid} and the total volume V_{total} of the investigated material.

$$\phi = \frac{V_{fluid}}{V_{tot}} \tag{2}$$

- *tortuosity* - α_∞ [−]: this dimensionless quantity evaluates the sinuous fluid paths through the material. It is defined as:

$$\alpha_\infty = \frac{\frac{1}{V}\int_V v^2 \mathrm{d}V}{\left|\frac{1}{V}\int_V \vec{v}\mathrm{d}V\right|^2} \tag{3}$$

  where v is the microscopic velocity of an inviscid fluid within the pores and V is the equivalent homogeneous fluid volume.

- *viscous and thermal characteristic lengths* - Λ, $\Lambda^{'}$ [μm]: these two quantities describe the viscous forces and the thermal exchanges between the solid frame and the saturated fluid contained in it. Their influence is significant at high frequencies. They are defined as:

$$\Lambda = 2\frac{\int_V |v(r)|^2 \mathrm{d}V}{\int_S |v(r)|^2 \mathrm{d}S} \tag{4}$$

$$\Lambda^{'} = 2\frac{\int_V \mathrm{d}V}{\int_S \mathrm{d}S} \tag{5}$$

  where V is the volume of the fluid contained within the pores and S is the interface surface between the solid frame and the fluid.

The effective density ρ of the porous material, which is associated to the inertial and viscous forces, can be determined as:

$$\rho = \frac{\alpha_\infty \rho_0}{\phi} + \frac{\sigma}{\mathrm{j}\omega}\sqrt{1 + \frac{4\mathrm{j}\alpha_\infty^2 \eta \rho_0 \omega}{\sigma^2 \Lambda^2 \phi^2}} \tag{6}$$

where ρ_0 is the air density and η its viscosity, while ω represents the angular frequency and $\mathrm{j} = \sqrt{-1}$ is the imaginary unit. The effective bulk modulus K takes into account the thermal exchanges between the frame and fluid, and it can be determined as:

$$K = \frac{\gamma P_0}{\phi}\left[\gamma - (\gamma - 1)\left(1 + \frac{8\eta}{\mathrm{j}\rho_0 \omega N_{Pr} \Lambda'^2}\sqrt{1 + \frac{\mathrm{j}\rho_0 \omega N_{Pr} \Lambda'^2}{16\eta}}\right)^{-1}\right] \tag{7}$$

being N_{Pr} the Prandtl number, γ the specific heat ratio and P_0 the static pressure. From the complex effective density ρ and the complex effective bulk modulus, given in Eq. (6) and (7) respectively, the characteristic impedance Z_c and the complex wavenumber k_c can be computed as:

$$Z_c = \sqrt{\rho K} \tag{8}$$

$$k_c = \omega\sqrt{\frac{\rho}{K}} \tag{9}$$

Considering a porous material of thickness h placed on a rigid reflecting boundary, the surface impedance for normal incidence Z_s can be determined as:

$$Z_s = -\mathrm{j}Z_c \cot(k_c h) \tag{10}$$

Table 1: Effective fluid dynamic radius of the hemp fibres determined at each stage of the manufacturing process.

	01.CAR	02.NaOH	03.WTC	04.FTC
$r_{effect,FD}$ [μm]	27.3	29.3	22.7	18.4

the normal incidence sound absorption coefficient α_n is finally evaluated as:

$$\alpha_n = \frac{4\mathrm{Re}\left\{\frac{Z_s}{\rho_0 c_0}\right\}}{\left|\frac{Z_s}{\rho_0 c_0}\right|^2 + 2\mathrm{Re}\left\{\frac{Z_s}{\rho_0 c_0}\right\} + 1} \tag{11}$$

where c_0 represents the speed of sound in air.

4. Proposed methodology

4.1. Single density material characterisation

In order to determine all five physical parameters of the hemp fibrous material at each stage of the manufacturing process, which are required as input data in the JCA model as described in the previous paragraph Eq. (1)–(5), an approach based on an equivalent effective radius has been used. As already mentioned in section 2, the large dispersion which characterises the fibres' diameter distribution obtained from SEM images would lead to highly inaccurate estimates of a weighted average radius. Moreover, it should also be considered that with a non-normal distribution, as we obtained for each material, the average value has no physical meaning and is not a representative value of the distribution. Therefore, in the proposed methodology, an equivalent effective radius was determined by using a different approach. Based on a fluid dynamic analysis, Tarnow [37] derived a relationship between the constant fibre radius r and the air flow resistivity σ, considering randomly distributed fibres and an air flow perpendicular to their axes:

$$\sigma = \frac{4\pi\eta}{b^2\left[0.64\ln\left(\frac{b^2}{\pi r^2}\right) - 0.737 + \frac{\pi r^2}{b^2}\right]} \tag{12}$$

the coefficient b can be computed from the ratio between the fibres' density ρ_g and the density of the fibrous material ρ_w as [29]:

$$b = r\sqrt{\pi\frac{\rho_g}{\rho_w}} \tag{13}$$

Therefore, being the air flow resistivity an easily measurable quantity, the effective radius r of an equivalent homogeneous material with single diameter fibres can be computed using a simple minimisation algorithm based on Eq. (12). To this purpose, samples of loose hemp fibres, resulting from each manufacturing process described in section 2, were tested in the acoustic laboratories of the University of Ferrara. For each sample, the air flow resistivity σ was measured by means of the alternate flow method, as described in the EN 29053:1993 standard [38]. The effective radius r obtained for each material is reported in Table 1. Moreover, the normal incidence sound absorption coefficient α_n was measured by using a well-established transfer function method in an impedance tube, according to the ISO 10534-2:1998 standard [39]. The cylindrical

Figure 3: Investigated hemp fibres: a) loose hemp fibres; b) a fibrous material sample is created within the test rig; c) metallic mesh used to restrain the fibres in the sample holder.

samples were prepared by compressing the loose hemp fibres into the sample holder of each measurement test rig, as shown in Figure 3. A coarse metallic mesh was used to restrain the fibres when compressed at a chosen rate, in order to obtain samples with a constant density and also to prevent any leakage around the edge. For each processing stage, three different measurements were performed; each time the sample was removed and reinserted in the test rig. The porosity ϕ of the fibrous material was computed from the mass of lose hemp fibres, the volume of the sample holder it was contained within and the density of the fibres, according to the relationship:

$$\phi = 1 - \frac{\rho_w}{\rho_g} \tag{14}$$

The density of the fibres was estimated from the literature: $\rho_g = 1300\ \mathrm{kg/m^3}$. The tortuosity can be evaluated as a function of the material porosity as [40]:

$$\alpha_\infty = \left(\frac{1}{\phi}\right)^{0.7659} \tag{15}$$

It is possible to estimate the thermal characteristic length Λ' as a function of the mean square radius of the hemp fibres r [31], evaluated from the measured air flow resistivity using Eq. 12 as:

$$\Lambda' = b - r \tag{16}$$

By knowing these four physical parameters, the viscous characteristic length Λ can be finally evaluated from the measured absorption coefficient α_n by using a well established inversion method [41].

4.2. Material characterisation varying the compression rate

The analysis was further extended to the investigation of the possibility to compute the physical parameters of hemp fibrous material with an arbitrary compression rate. For example, the formulations developed by Castagnède et al. [31], both for 1D and 2D compression, allow to evaluate all five physical parameters for any compression rate $n = \rho_{w,(n)}/\rho_{w,(0)}$ by knowing the material's characteristics for a given density $\rho_{w,(0)}$ and thickness $h_{(0)}$. The great advantage of this approach is certainly represented by the fact that it can be easily applied in practical contexts, requiring few simple experimental measurements. However, it should be mentioned that the linear relationships, developed for 1D compression, have been validated only for a material with high internal porosity within the range $\phi = 0.944 \div 0.995$. In fact, it has been shown [42, 43] that Castagnède et al.'s formulas for 1D compression provide reliable results when a small compression rate and highly porous materials are considered, although it may be inaccurate to investigate high density materials. Moreover, this approach does not take into account the variation of the fibres' orientation due to the compression, which has been proven to have a significant influence on the physical properties of the material [43]. Nevertheless, Castagnède's model, due to its simplicity and straightforward applicability, represents a good starting point to define an empirical tool to be used in order to characterise hemp fibres, which have never been systematically analysed before from an acoustic point of view. To this purpose, the linear relationships associated to mono-axial 1D compression, to define the physical parameters of the JCA model, have been used. However, a correction coefficient has been introduced as exponential of the compression rate in the air flow resistivity formulation. Instead of the linear relationship proposed by Castagnède for 1D compression, the compression rate n is raised to the power of $A = 2.1337$. Such coefficient was determined though a least square minimisation of the percentage error between the computed air flow resistivity and the experimental data, measured on samples of five different thicknesses for each investigated material. Indicating with the subscript $_{(0)}$ the initial set of physical parameters, determined as described in the previous section, the air flow resistivity of hemp fibrous material at any given compression rate n, indicated with the subscript $_{(n)}$, was evaluated as:

$$\sigma_{(n)} = n^{A}\sigma_{(0)} \tag{17}$$

It should be mentioned that an alternative set of equations, developed using numerical fluid analyses, assuming that only the air filling the porosity changes during compression while the cross-sectional area of the fibres remains undeformed (which is equivalent to the assumptions adopted by Castagnède for 1D compression), was also recently presented by Hirosawa and Nakagawa [44]. In this case the airflow resistivity does not vary linearly with the compression rate, even though, as will be shown in the next section, this equation does not provide accurate results at the higher densities either. The other physical parameters of the hemp fibrous material, such as its tortuosity α_∞, and its viscous and thermal characteristic lengths Λ and $\Lambda^{'}$, were computed for a varying compression rate by using Castagnède's formulations:

$$\alpha_{\infty,(n)} = 1 - n\left(1 - \alpha_{\infty,(0)}\right) \tag{18}$$

$$\Lambda_{(n)} = \frac{\Lambda_{(0)}}{n^{1/2}} + r\left(\frac{1}{n^{1/2}} - 1\right) \tag{19}$$

$$\Lambda^{'}_{(n)} = \frac{\Lambda^{'}_{(0)}}{n^{1/2}} + r\left(\frac{1}{n^{1/2}} - 1\right) \tag{20}$$

The material's porosity was determined as the ratio between the material's density and the fibres' density, as provided in Eq. (14); alternatively it can also be expressed as:

$$\phi_{(n)} = 1 - n\left(1 - \phi_{(0)}\right) \tag{21}$$

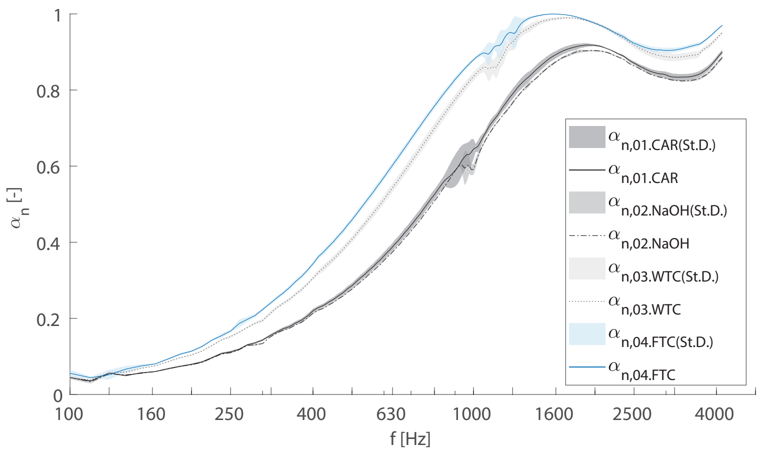

Figure 4: Normal incidence sound absorption coefficient measured on hemp fibre samples, with thickness h = 40 mm and density ρ_w = 88 kg/m^{3}at the four different stages of the manufacturing process.

The hemp fibrous material was characterised for any compression rate within the range $n = 0.5 \div 2$, starting from the physical parameters determined as a function of the fluid dynamic effective radius for the material with density $\rho_{w,(0)}$ = 88 kg/m^3 and thickness $h_{(0)}$ = 40 mm.

5. Results and validation

The way in which each manufacturing process, presented in section 2, affects the acoustic performance of the material was analysed by comparing the normal incidence sound absorption coefficient α_n, measured on samples of loose hemp fibres at the four different stages of the process, with identical density ρ = 88 kg/m^3 and thickness h = 40 mm. The sound absorption measurements were performed, as described in section 4, three times for each sample; the experimental standard deviation is reported as a shaded area around the average curve of the associated absorption coefficient. As shown in Figure 4, there is no relevant difference between the fibres only carded 01.CAR and the fibres which also went through the alkaline treatment 02.NaOH. In fact, even though the sound absorption coefficient associated with the 02.NaOH fibres is slightly lower than the values related to the carded fibres 01.CAR, these differences are barely noticeable and the two curves almost superpose within the entire frequency range. On the other hand, the alkaline treatment 02.NaOH combined with the wide tooth combing 03.WTC significantly increases the sound absorption of the material. This effect is due to the noteworthy reduction of the mean diameter caused by a substantial morphological change of the fibre structure. In fact, only the combination of the elimination of non-cellulosic components (02.NaOH) combined with a mechanical treatment (03.WTC) allows the opening of the bundles and the release of the fibrils that have a smaller diameter. The acoustic performance of the hemp fibrous material is slightly further enhanced after the fine tooth combing treatment 04.FTC, which allows the natural fibrous material to match the normal incidence sound absorption of traditional synthetic fibres.

Table 2: Physical parameters of the hemp fibrous materials used as initial data set to characterise the material properties at varying compression rate

	01.CAR	02.NaOH	03.WTC	04.FTC
$h_{(0)}$ [mm]	40	40	40	40
$\rho_{(0)}$ $\left[\mathrm{kg/m^3}\right]$	88	88	88	88
$\phi_{(0)}$ $[-]$	0.93	0.93	0.93	0.93
$\sigma_{(0)}$ $\left[Pas/m^2\right]$	5536	4920	7883	12503
$\alpha_{\infty,(0)}$ $[-]$	1.05	1.05	1.05	1.05
$\Lambda_{(0)}$ $[\mu\mathrm{m}]$	109	115	59	50
$\Lambda'_{(0)}$ $[\mu\mathrm{m}]$	160	170	135	109

The characterisation methodology described in the previous section was validated by comparing the physical parameters, computed for a varying compression rate n, with experimental results. The initial set of material properties, provided in Table 2, was computed as a function of the effective radius, derived from the experimental air flow resistivity $\sigma_{(0)}$, or from the normal incidence sound absorption coefficient $\alpha_{n,(0)}$; both measured on samples of hemp fibres 40 mm thick, with a density of $\rho_{(0)} = 88$ kg/m^3. In order to validate the results, additional measurements were made on the hemp fibrous material at each stage of the manufacturing process. In particular, a total of five different densities ρ_w were experimentally tested within the range $\rho_{w,i} = 59 \div 141$ kg/m^3, obtaining hemp fibrous samples with a thickness varying from $h = 60$ mm to $h = 25$ mm. For each sample the normal incidence absorption coefficient and the air flow resistivity were experimentally measured as described in section 4. Moreover, the materials' tortuosity α_∞ was assessed from an ultrasonic experimental method [45], while the viscous Λ and thermal characteristic lengths Λ' were evaluated by using well consolidated inversion techniques based on a least mean square algorithm [41].

Figure 5 shows the experimental air flow resistivity, measured on samples of the fibrous material, with five different densities, after each processing step. Results were found to be consistent with the sound absorption coefficients, shown in Figure 4. In fact, for all the investigated densities the fibres resulting from the process 04.FTC exhibit the higher air flow resistivity, while the lowest values are associated with the fibres resulting from the alkaline treatment 02.NaOH; this behaviour is more emphasised as the density increases. An increase in air flow resistivity is thus associated with an improvement of the material's absorption coefficient. The experimental air flow resistivity, plotted together with the error bars representing the experimental standard deviation, are compared in Figure 5, with the air flow resistivity computed for a varying compression rate $n = 0.5 \div 2$, according to Eq. (17). For each material a good agreement is found between the experimental results and the curve computed using the formulation proposed in this paper $\sigma_{i,(n)}$. The results obtained from the linear model proposed by Castagnède for 1D compression is also reported as a dotted line $\sigma_{i,(n,1D)}$, in order to demonstrate how it is not suitable for this kind of material, providing inaccurate results which progressively deviate from the experimental evidence as the density increases. The air flow resistivity $\sigma_{i,(n,H)}$ computed using the non-linear equation

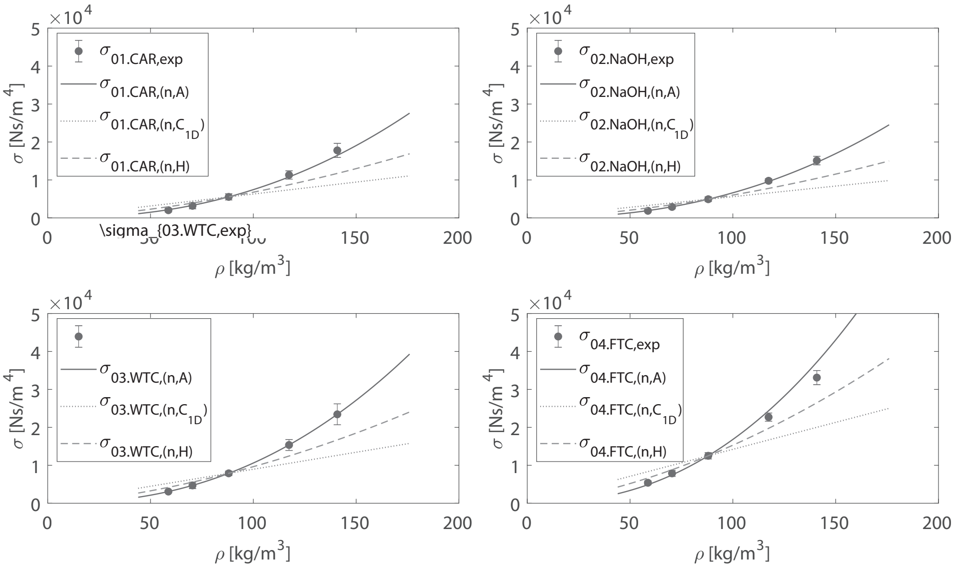

Figure 5: Experimental and estimated air flow resistivity evaluated at each stage of the manufacturing process on samples of various densities at the four manufacturing stages: (a) carding process: 01.CAR; (b) alkaline treatment: 02.NaOH; (c) wide tooth combing: 03.WTC; (d) fine tooth combing: 04.FTC.

developed by Hirosawa et al. is also reported. A slightly better agreement is found for a low compression rate. Nevertheless, at the higher densities it clearly deviates from the experimental results.

On the other hand, Castagnède's equation for 1D compression, which in this case is equivalent to the one developed by Hirosawa, provides a good approximation of the experimental tortuosity, as shown in Figure 6. However, the curve obtained from the linear relationship for 1D compression slightly deviates from the experimental results at the highest densities. It should be considered that such differences are comparable with the experimental standard deviation, reported as error bars; besides, such variations have a negligible influence on sound absorption performance.

It was not possible to measure the viscous and the thermal characteristics lengths. These quantities were thus determined, for each material, by using a consolidated inversion technique, minimising the difference between the experimental sound absorption coefficient and the results obtain from the JCA model [41].

However, keeping in mind that at the low frequencies, or for materials with a low density, both the viscous and the thermal characteristics lengths do not have a significant influence on the sound absorption coefficient, it is evident in these cases the inversion technique would not necessarily provide the best physical solution. A sensitivity analysis of these quantities on the JCA model, was carried out as a function of the material density. Numerical results were compared with all the values of Λ and $\Lambda^{'}$, obtained from the minimisation algorithm, which guarantee an absorption coefficient within 3% of error with respect to the experimental sound absorption coefficient. . As shown in Figure 7, the standard deviation associated with the characteristic viscous length, plotted as a shaded area around the best fit results, is very limited for all four materials,

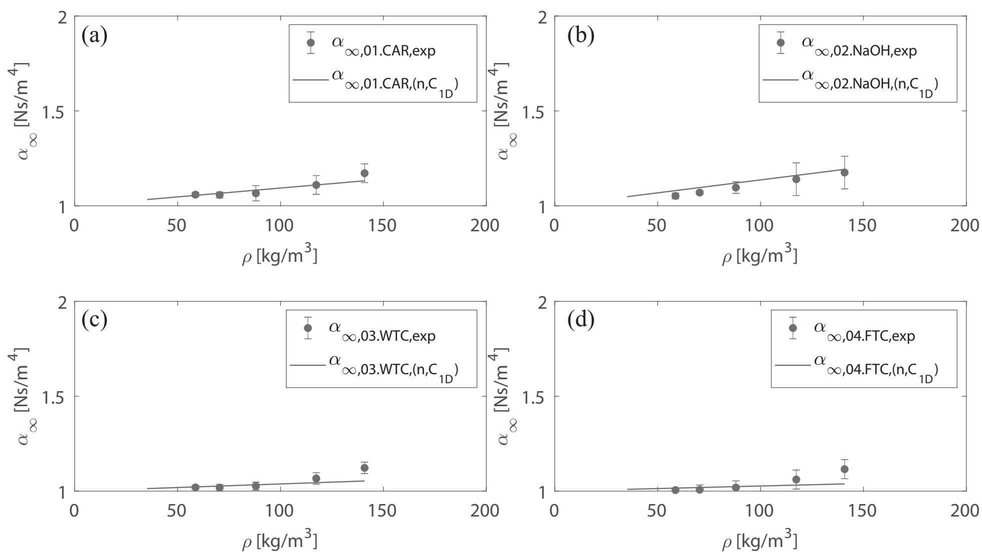

Figure 6: Experimental and estimated tortuosity evaluated on samples of various densities at the four manufacturing stages: (a) carding process: 01.CAR; (b) alkaline treatment: 02.NaOH; (c) wide tooth combing: 03.WTC; (d) fine tooth combing: 04.FTC.

both for high and low densities. However, as the porosity increases, the influence of the fluid viscosity is more significant and the standard deviation decreases further. The numerical curve for a varying compression rate $\Lambda_{(n,1D)}$, given in Figure 7, is in good agreement with the experimental values of the material resulting from the two last manufacturing processes: 03.WTC and 04.FTC. However, it significantly deviates from the characteristic viscous length evaluated from experimental data for the fibres which underwent only the first two manufacturing treatments: 01.CAR and 02.NaOH. As shown in Figure 8, an analogous picture can be drawn comparing the thermal characteristic length derived from the experimental data set and the numerical curve evaluated for a varying compression rate. As was found for the viscous characteristic length, Castagnède's equation for 1D compression provides an accurate approximation for the materials obtained from the last two manufacturing processes: 03.WTC and 04.FTC, while relevant discrepancies are found for the materials at the first two stages: 01.CAR and 02.NaOH. However, by looking at results obtained from the inversion algorithm, considering all the solutions which provide an absorption coefficient within 3% error, a huge standard deviation is found. This means that the thermal characteristic length does not significantly affect the sound absorption coefficient of materials with high porosity or with rough fibres.Although the numerical results deviate from the best value solution, represented by black circles, were well within the shaded area which represents the standard deviation obtained in the minimisation approach. Both characteristics lengths were also computed at a varying compression rate by using the formulations provided by Hirosawa, which, unlike in Castagnède's model, do not depend on the effective radius of the fibres. These results are indicated in Figures 7 and 8 as $\Lambda_{(n,H)}$ and $\Lambda'_{(n,H)}$ respectively. Even though small differences are observed, this model does not provide a significant better accuracy compared to experimental results.

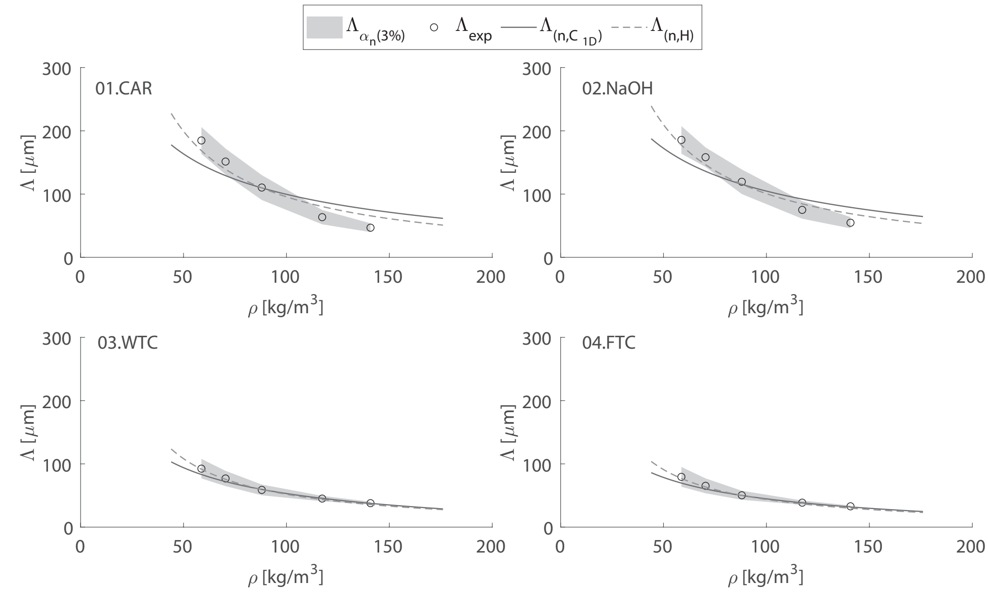

Figure 7: Experimental determined from inversion technique and estimated characteristic viscous length evaluated on samples of various densities at the four manufacturing stages: (a) carding process: 01.CAR; (b) alkaline treatment: 02.NaOH; (c) wide tooth combing: 03.WTC; (d) fine tooth combing: 04.FTC.

Finally, in order to determine whether the accuracy provided by this approach may guarantee a good approximation of the material's acoustic performance, the experimental sound absorption form normal incidence α_n, measured at each stage of the manufacturing process for five different compression rates, was compared to the results obtained from the JCA model. The physical parameters, numerically computed for a varying compression rate, were used as input data in the model. As shown in Figure 9, a good agreement is found between the numerical results and the experimental sound absorption for all four materials and for each of the investigated compression rates. Since the small discrepancies highlighted in some cases between numerical and experimental curves are comparable with the experimental standard deviation found between different measurements of the same sample, shown in Figure 4, it can be concluded that the characterisation approach investigated in this study provides an accurate estimation of the physical parameters required to describe the acoustic performance of hemp fibre materials using the JCA model.

6. Conclusion

A study regarding the acoustic performance of hemp fibrous materials and the physical parameters by which it is affected has been presented. An analysis was carried out of how to optimise the manufacturing process in order to obtain a natural, sustainable and renewable fibrous material, which can provide a sound absorbing performance comparable that provided by traditional synthetic fibres. An experimental investigation on hemp-fibres identified the influence of each stage of the manufacturing process both on the acoustic performance and on the physical

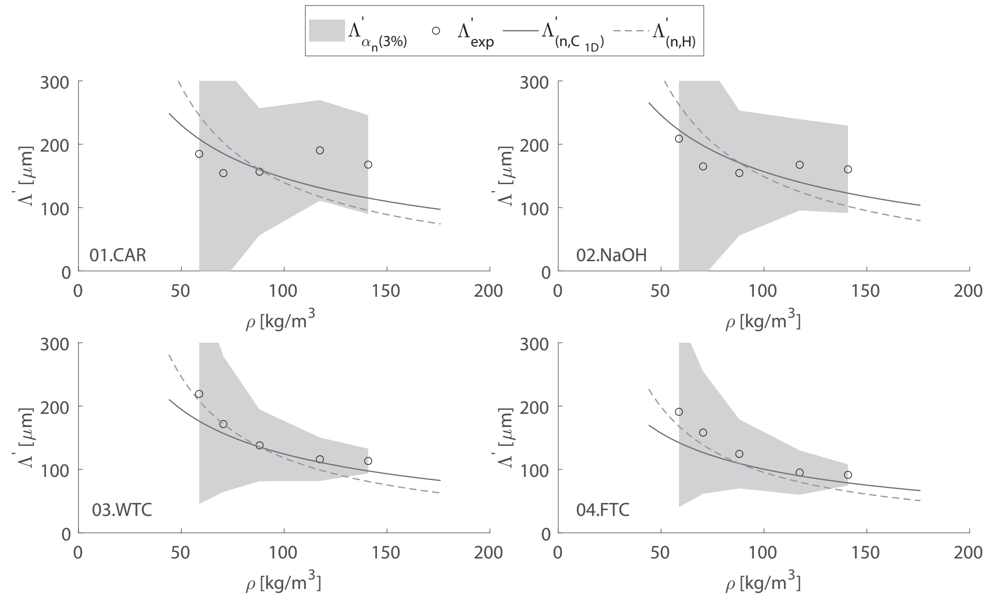

Figure 8: Experimental determined from inversion technique and estimated characteristic thermal length evaluated on samples of various densities at the four manufacturing stages: (a) carding process: 01.CAR; (b) alkaline treatment: 02.NaOH; (c) wide tooth combing: 03.WTC; (d) fine tooth combing: 04.FTC.

characteristics of the fibrous material. It was shown that an alkaline treatment (02.NaOH) performed on the material after the carding process (01.CAR) does not significantly affect either its acoustic performance or its physical properties, such as the airflow resistivity for example, unless this is followed by two combing processes. The first one is made with a wide tooth comb, while the second with a finer one. These processes allow to improve the material acoustic performance, by increasing air flow resistivity and reducing the effective radius of the fibres. The first combing represents a fundamental step of the process, while the last one is a refinement which allows a small further improvement of the performance. From a physical point of view, the combing process, performed after alkaline treatment, modifies the morphology of the fibre by promoting the opening of the bundles and freeing the fibrils. These substructures are in fact characterized by a smaller diameter. The physical parameters required to describe the hemp fibres using the JCA equivalent fluid model were characterised after each manufacturing procedure. Since natural fibres are characterised by large variability the distribution of diameters, the proposed approach is based on the concept of effective equivalent fluid-dynamic radius, derived from the experimental air flow resistivity by using the model developed by Tarnow. Besides, a simplified methodology to investigate the acoustic performance of hemp fibrous materials, as a function of the material density, was then proposed, providing a useful tool to compute and compare the sound propagation into the material with different degrees of compression. The properties of the hemp fibrous material for a varying compression rate were evaluated with good accuracy by using the simple model developed by Castagnède for mono-axial compression, from the parameters characterised for a given density, by means of a fluid-dynamic approach. However, in order to consider also materials with a high compression rate, i.e. high density and low porosity, or aspects which are not taken into account in this simplified model, such as the fibres' orientation, the 1D linear equation provided to compute the air flow resistivity was modified by introducing an exponential correction coefficient. Such term was determined from the airflow resistivity measured on hemp fibre samples at different compression rates by means of a minimisation algorithm. At each manufacturing stage, all of the investigated parameters numerically evaluated were validated by comparison with the experimental results, measured on hemp fibre samples with five different densities and thicknesses. More specifically, the air flow resistivity, the tortuosity and the normal incidence sound absorption were directly measured, while the viscous and thermal characteristic lengths were determined from the experimental data set using an inversion technique. The validation highlighted a good agreement between the results obtained from the proposed methodology and the experimental physical parameters. Due to the simplified and practical nature of the proposed approach some discrepancies were found, especially at the highest densities and for the materials with rough fibres, such as the ones obtained from the first two stages of the manufacturing process. However, the differences found between the experimental and numerical results were comparable with the experimental standard deviation obtained from different measurements of the same sample. Moreover, numerically evaluated parameters used as input data in the Johnson-Champoux-Allard model provided a very good approximation of the experimental sound absorption coefficient measured at each stage of the manufacturing process on materials at five different compression rates. The proposed model can certainly be refined in the follow-up of this project, even though this simplified approach represents a simple and reliable tool to analyse the acoustic performance of hemp fibrous materials, which has not been investigated before.

Acknowledgement

The authors are grateful to Mr. Jonathan Vallari of EmilCanapa for providing the hemp fibres used in this study.

References

References

[1] F. Ardente, M. Beccali, M. Cellura, M. Mistretta, Building energy performance: a lca case study of kenaf-fibres insulation board, Energy and Buildings 40 (1) (2008) 1–10.

[2] S. V. Joshi, L. Drzal, A. Mohanty, S. Arora, Are natural fiber composites environmentally superior to glass fiber reinforced composites?, Composites Part A: Applied science and manufacturing 35 (3) (2004) 371–376.

[3] C. Zhou, S. Q. Shi, Z. Chen, L. Cai, L. Smith, Comparative environmental life cycle assessment of fiber reinforced cement panel between kenaf and glass fibers, Journal of Cleaner Production 200 (2018) 196–204.

[4] C. Ingrao, A. L. Giudice, J. Bacenetti, C. Tricase, G. Dotelli, M. Fiala, V. Siracusa, C. Mbohwa, Energy and environmental assessment of industrial hemp for building applications: A review, Renewable and Sustainable Energy Reviews 51 (2015) 29–42.

[5] E. Awwad, M. Mabsout, B. Hamad, M. T. Farran, H. Khatib, Studies on fiber-reinforced concrete using industrial hemp fibers, Construction and Building Materials 35 (2012) 710–717.

[6] H.-R. Kymäläinen, A.-M. Sjöberg, Flax and hemp fibres as raw materials for thermal insulations, Building and environment 43 (7) (2008) 1261–1269.

[7] A. Bourdot, T. Moussa, A. Gacoin, C. Maalouf, P. Vazquez, C. Thomachot-Schneider, C. Bliard, A. Merabtine, M. Lachi, O. Douzane, et al., Characterization of a hemp-based agro-material: Influence of starch ratio and hemp shive size on physical, mechanical, and hygrothermal properties, Energy and Buildings 153 (2017) 501–512.

[8] F. Iucolano, B. Liguori, P. Aprea, D. Caputo, Thermo-mechanical behaviour of hemp fibers-reinforced gypsum plasters, Construction and Building Materials 185 (2018) 256–263.

Published article available online: https://doi.org/10.1016/j.apacoust.2019.02.022

[9] E. Sassoni, S. Manzi, A. Motori, M. Montecchi, M. Canti, Novel sustainable hemp-based composites for application in the building industry: Physical, thermal and mechanical characterization, Energy and Buildings 77 (2014) 219–226.

[10] G. Costantine, C. Maalouf, T. Moussa, G. Polidori, Experimental and numerical investigations of thermal performance of a hemp lime external building insulation, Building and Environment 131 (2018) 140–153.

[11] B. Moujalled, Y. A. Oumeziane, S. Moissette, M. Bart, C. Lanos, D. Samri, Experimental and numerical evaluation of the hygrothermal performance of a hemp lime concrete building: A long term case study, Building and Environment 136 (2018) 11–27.

[12] A. Santoni, P. Bonfiglio, F. Mollica, P. Fausti, F. Pompoli, V. Mazzanti, Vibro-acoustic optimisation of wood plastic composite systems, Construction and Building Materials 174 (2018) 730–740.

[13] F. Asdrubali, S. Schiavoni, K. Horoshenkov, A review of sustainable materials for acoustic applications, Building Acoustics 19 (4) (2012) 283–311.

[14] F. Asdrubali, F. D'Alessandro, S. Schiavoni, A review of unconventional sustainable building insulation materials, Sustainable Materials and Technologies 4 (2015) 1–17.

[15] U. Berardi, G. Iannace, Predicting the sound absorption of natural materials: Best-fit inverse laws for the acoustic impedance and the propagation constant, Applied Acoustics 115 (2017) 131–138.

[16] A. Santoni, P. Bonfiglio, J. L. Davy, P. Fausti, F. Pompoli, L. Pagnoncelli, Sound transmission loss of ETICS cladding systems considering the structure-borne transmission via the mechanical fixings: Numerical prediction model and experimental evaluation, Applied acoustics 122 (2017) 88–97.

[17] S. Secchi, G. Cellai, P. Fausti, A. Santoni, N. Zuccherini Martello, Sound transmission between rooms with curtain wall facades: a case study, Building Acoustics 22 (3-4) (2015) 193–207.

[18] N. Zuccherini Martello, F. Aletta, P. Fausti, J. Kang, S. Secchi, A psychoacoustic investigation on the effect of external shading devices on building façades, Applied Sciences 6 (12) (2016) 429.

[19] M. Delany, E. Bazley, Acoustical properties of fibrous absorbent materials, Applied acoustics 3 (2) (1970) 105–116.

[20] Y. Miki, Acoustical properties of porous materials-modifications of delany-bazley models, Journal of the Acoustical Society of Japan (E) 11 (1) (1990) 19–24.

[21] D. L. Johnson, J. Koplik, R. Dashen, Theory of dynamic permeability and tortuosity in fluid-saturated porous media, Journal of fluid mechanics 176 (1987) 379–402.

[22] Y. Champoux, J.-F. Allard, Dynamic tortuosity and bulk modulus in air-saturated porous media, Journal of applied physics 70 (4) (1991) 1975–1979.

[23] D. Lafarge, P. Lemarinier, J. F. Allard, V. Tarnow, Dynamic compressibility of air in porous structures at audible frequencies, The Journal of the Acoustical Society of America 102 (4) (1997) 1995–2006.

[24] M. Garai, F. Pompoli, A simple empirical model of polyester fibre materials for acoustical applications, Applied Acoustics 66 (12) (2005) 1383–1398.

[25] U. Berardi, G. Iannace, Acoustic characterization of natural fibers for sound absorption applications, Building and Environment 94 (2015) 840–852.

[26] C. Piégay, P. Gle, E. Gourdon, E. Gourlay, S. Marceau, Acoustical model of vegetal wools including two types of fibers, Applied Acoustics 129 (2018) 36–46.

[27] H. Mamtaz, M. H. Fouladi, M. Al-Atabi, S. Narayana Namasivayam, Acoustic absorption of natural fiber composites, Journal of Engineering 2016.

[28] Z. Lim, A. Putra, M. Nor, M. Yaakob, Sound absorption performance of natural kenaf fibres, Applied Acoustics 130 (2018) 107–114.

[29] V. Tarnow, Measurement of sound propagation in glass wool, The Journal of the Acoustical Society of America 97 (4) (1995) 2272–2281.

[30] P. Shravage, P. Bonfiglio, F. Pompoli, et al., Hybrid inversion technique for predicting geometrical parameters of porous materials, Journal of the Acoustical Society of America 123 (5) (2008) 3284.

[31] B. Castagnede, A. Aknine, B. Brouard, V. Tarnow, Effects of compression on the sound absorption of fibrous materials, Applied Acoustics 61 (2) (2000) 173–182.

[32] M. Horne, Bast fibres: hemp cultivation and production, in: Handbook of Natural Fibres: Types, Properties and Factors Affecting Breeding and Cultivation, Elsevier, 2012, pp. 114–145.

[33] L. Y. Mwaikambo, M. P. Ansell, Chemical modification of hemp, sisal, jute, and kapok fibers by alkalization, Journal of applied polymer science 84 (12) (2002) 2222–2234.

[34] J. Zhang, H. Zhang, J. Zhang, Effect of alkali treatment on the quality of hemp fiber., Journal of Engineered Fabrics & Fibers (JEFF) 9 (2).

[35] V. Mazzanti, A. Bonanno, F. Mollica, G. Filippone, Influence of alkaline treatment on hemp fibers filled poly (lactic acid), in: AIP Conference Proceedings, Vol. 1981, AIP Publishing, 2018, p. 020016.

[36] H. T. Luu, R. Panneton, C. Perrot, Effective fiber diameter for modeling the acoustic properties of polydisperse fiber networks, The Journal of the Acoustical Society of America 141 (2) (2017) EL96–EL101.

[37] V. Tarnow, Airflow resistivity of models of fibrous acoustic materials, The Journal of the Acoustical Society of

America 100 (6) (1996) 3706–3713.

[38] EN 29053 – Acoustics - Materials for acoustical applications - Determination of airflow resistance, Standard, European Committee for Standardisation, Brussels, Belgium (1993).

[39] ISO 10534-2 – Acoustics – Determination of sound absorption coefficient and impedance in impedance tubes – Part 2: Transfer-function method., Standard, International Organization for Standardization, Geneva, CH (1998).

[40] H. T. Luu, C. Perrot, R. Panneton, Influence of porosity, fiber radius and fiber orientation on the transport and acoustic properties of random fiber structures, Acta Acustica united with Acustica 103 (6) (2017) 1050–1063.

[41] P. Bonfiglio, F. Pompoli, Inversion problems for determining physical parameters of porous materials: Overview and comparison between different methods, Acta Acustica united with Acustica 99 (3) (2013) 341–351.

[42] B. Campolina, N. Dauchez, N. Atalla, O. Doutres, Effect of porous material compression on the sound transmission of a covered single leaf panel, Applied Acoustics 73 (8) (2012) 791–797.

[43] L. Lei, N. Dauchez, J. Chazot, Prediction of the six parameters of an equivalent fluid model for thermocompressed glass wools and melamine foam, Applied Acoustics 139 (2018) 44–56.

[44] K. Hirosawa, H. Nakagawa, Formulae for predicting non-acoustical parameters of deformed fibrous porous materials, The Journal of the Acoustical Society of America 141 (6) (2017) 4301–4313.

[45] P. Bonfiglio, F. Pompoli, et al., Frequency dependent tortuosity measurement by means of ultrasonic tests, in: Proceeding of the 14^{th} International Congress on Sound and Vibration, Vol. 14, ICSV, Cairns, Australia, 2007, pp. 1–6.

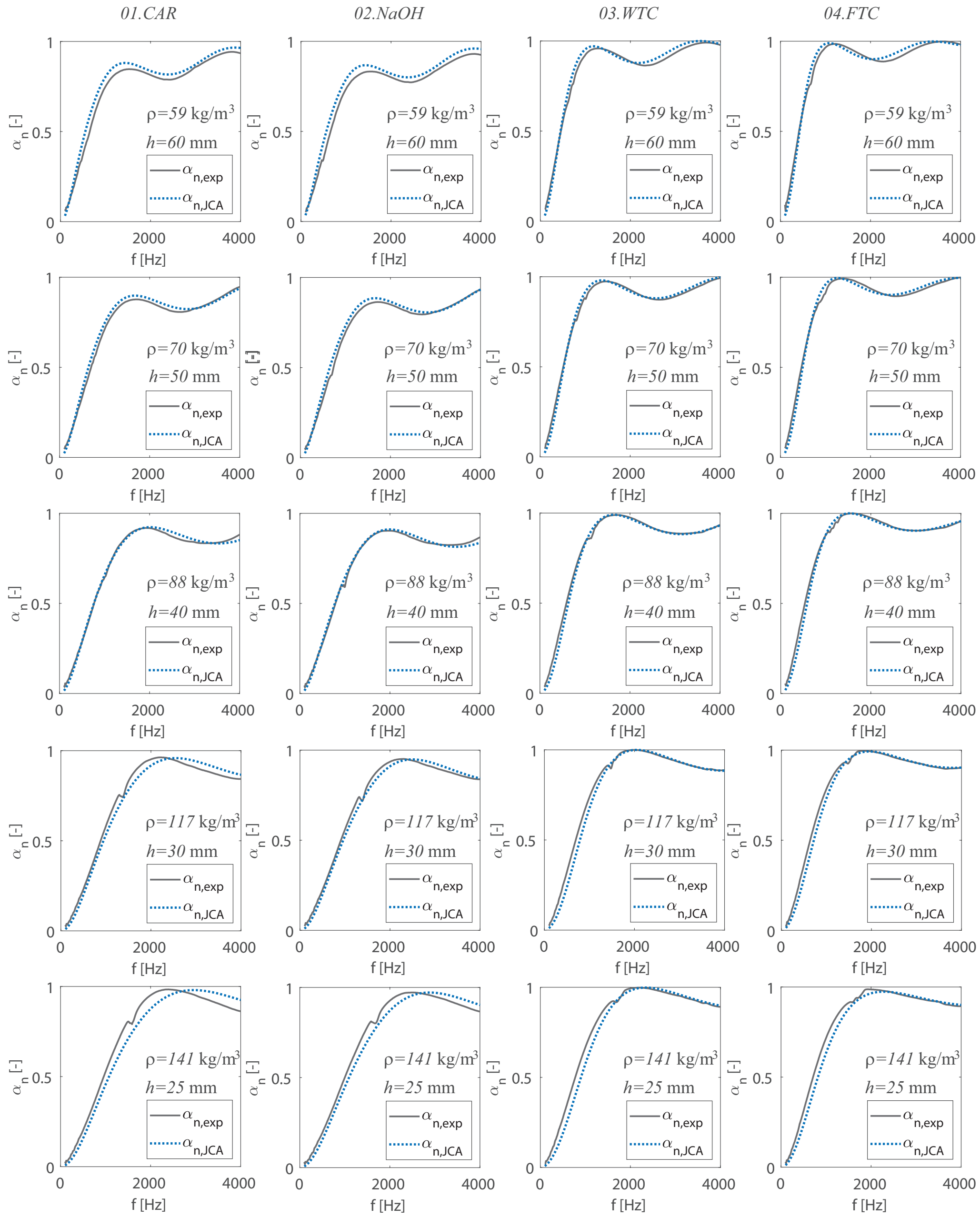

Figure 9: Comparison between numerical and experimental normal incidence sound absorption coefficient of the hemp fibrous material at each stage of the manufacturing process, for different compression rate.